Interfacial Mass and Heat Transfer During Evaporation:

I. An Experimental Technique and Some Results with a Clean Water Surface

URI NAVON and JOHN B. FENN

Princeton University, Princeton, New Jersey

A vacuum sweeper probe of a type introduced by previous investigators was evaluated for use in the study of heat and mass transfer during evaporation. A simple theory of the probe behavior was formulated and checked by experimental measurements over a substantial range of operating conditions. The results revealed that in the interpretation of experimental data the validity of some assumptions usually made is strongly dependent upon seemingly minor features of probe construction and operation. Errors as large as 200% were encountered when the gas flow distribution in the probe was not symmetrical. Consequently, some results now in the literature are open to question.

To test the technique and theory as well as to introduce a subsequent study of the effect of monolayers on evaporation, the evaporation rate from a clean water surface was measured over a temperature range of 2° to 22°C. The role of natural convection was clearly reflected in the increase of Nusselt number as the water bulk temperature passed through the density inversion at 4°C. A relation between Nusselt and Rayleigh numbers was determined and found to be consistent with earlier results of others.

The process by which water evaporates into an inert gas has received much attention in the last two decades. To a large extent many studies have been motivated by increasing interest in evaporation control and in the potential use of monomolecular films to inhibit loss of water from reservoirs (*1, 2*). Moreover, much of this previous work was concerned mainly with gas-phase diffusional resistance or with surface resistance and its dependence upon the presence of surface films. Resistance due to heat transfer in the bulk water, and in particular the role of natural convection resulting from evaporative cooling of the surface, have not received much attention. Jarvis (*3*) measured surface temperature during evaporation. Schlieren techniques were used by Spangenberg and Rowland to visualize convective flow initiated at the surface (*4*) and by Berg, Boudart, and Acrivos to study convection driven by both buoyancy and surface-tension mechanisms (*5*). In contrast to this relatively small effort, the phenomenon of natural convection in liquid layers without evaporation has been studied extensively since Benard's experiments at the turn of the century (*6*).

The investigation reported here was done as the first part of a study of the effect of monomolecular films on the evaporation of water. The approach was based on the unique reversal in the density-temperature relation which occurs at 4°C. and which marks a change in the heat transfer mode (*7* to *9*). From simultaneous measurements of evaporation rates and temperature profiles at temperatures above and below 4°C., it was hoped that the resistance to heat transfer with and without natural convection could be determined. In this way the role of natural convection might be quantitatively characterized. It was clear at the outset that the measurement of evaporation rate would be of critical importance. Consequently, a great deal of attention was first directed to the development and critical examination of methods and techniques. The results of this preliminary report were somewhat surprising and of intrinsic interest and importance. They provide the basis of the present work. The results with monomolecular films will be presented in a subsequent paper.

APPARATUS AND PROCEDURE

In previous measurements of evaporation rates into ambient gas from a quiescent water surface, one of two principal variations in technique was used. In the first the increase in weight with time was determined for a dessicant placed near the surface (*2, 10*). Because the evaporated molecules had to diffuse through a stagnant gas layer, this method resulted in a relatively high overall resistance to evaporation. In the second variation a stream of dry gas was allowed to flow gently over the surface by means of a specially designed probe. The evaporation rate was obtained by determining the amount of water picked up by the gas (*11*). In the first use of such a vacuum sweeper probe, the water content of the gas was determined by passing it through a drying tube whose weight increase could be measured. In more recent work a thermal conductivity cell was used to determine the water content of the probe gas (*12*). A flow rate determination thus permitted an instantaneous measure of the evaporation rate. This modification provided a fast response and opened the way for a determination of desorption rates for gases in solution (*13*). However, the need for expensive helium or dangerous hydrogen as the carrier gas is a disadvantage. In the present study a further modification of the flowing gas method was introduced by incorporating a commercially available moisture analyzer (CEC Model 26-303) to monitor the water content of the probe gas. This analyzer is a coulometric device through which a gas sample flows at a fixed rate. All of the water vapor present in the gas is absorbed and electrolyzed. The electrolysis current is continuously recorded and indicates the moisture content of the gas. The advantages of the device include its high sensitivity and its specificity to water so that any carrier gas can be used. In the present study most of the measurements were done with nitrogen.

The evaporation probe is shown schematically in Figure 1. It consisted of a stainless steel tube (22.2 mm. I.D.) surrounding a solid Teflon cylinder containing a 1-mm. center hole through which the sampled gas was withdrawn. The primary flow of carrier gas was introduced through a 1-mm. annu-

John B. Fenn is at Yale University, New Haven, Connecticut. Uri Navon is at the Technion, Haifa, Israel.

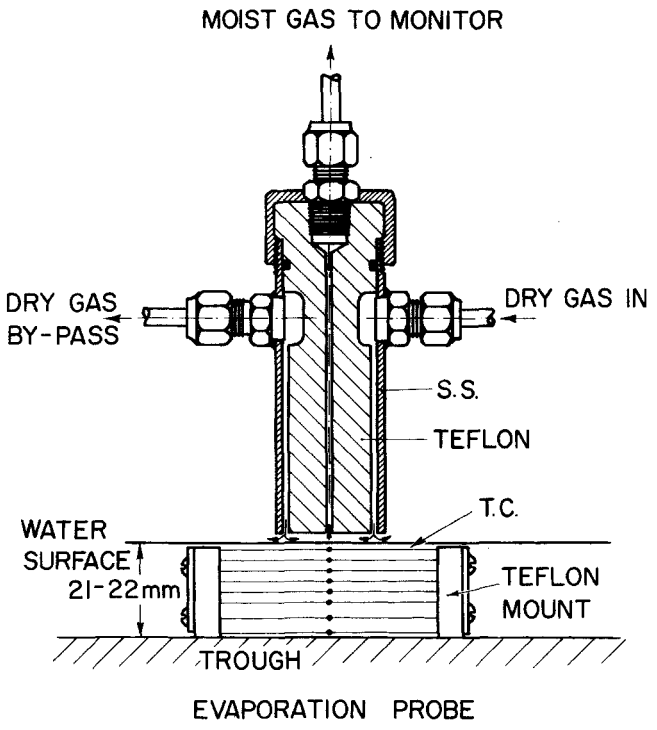

Fig. 1. Evaporation probe and thermocouple assembly.

lar gap between the outer tube and the Teflon cylinder. The tube and cylinder were kept in precise coaxial position by three set screws in the tube wall. The importance of this provision will emerge in later discussion. In the configuration used by previous investigators the lower surface of the Teflon cylinder was recessed 1 mm. relative to the plane defined by the lower end of the outer tube. For some tests, which will be described, the same recessed configuration was used in the present work. Most of the results were obtained with no recess. That is, the lower surface of the Teflon cylinder was coplanar with the lower end of the outer tube.

When in use the probe was placed so that the lower surface of the Teflon cylinder was about 2 mm above the water surface. Dry gas at a measured rate of flow was introduced through the annulus toward the water. A portion of the annular flow passed over the surface of the water and was withdrawn through the center hole in the teflon cylinder. The remainder flowed radially outward, forming a barrier to inward diffusion of external water vapor. At the relatively high evaporation rates often encountered, the water content of the gas leaving the probe through the center hole was far above the 1,000 p.p.m. limit which the monitor could tolerate at the recommended flow rate of 100 cu. cm./min. In order to overcome this difficulty, the gas withdrawn from the probe was diluted by a metered stream of dry gas. The use of Teflon tubing throughout the flow system minimized spurious effects due to sorption or desorption of water at the tube walls.

The body of water from whose surface evaporation was measured was contained in a Teflon-coated trough 50 cm x 14 cm. x 2 cm. The trough was machined from an aluminum block and had walls about 1 cm. thick. Temperature distribution beneath the probe was determined by an array of seven thermocouples stretched between the two legs of a horizontal U-shaped mount, as shown in Figure 1. The thermocouples measured the electromotive force relative to a reference junction located in the bulk water in a region unaffected by the evaporation. The temperature of the reference junction was determined by measuring the electromotive force relative to an ice-bath junction. This arrangement provided a high sensitivity in the relative values of the temperature, which, for determining temperature gradients, was more important than high precision in the absolute values. The thermocouple outputs were recorded on the same chart with the moisture content. The trough and the probe were contained in a thermostatically controlled enclosure which could maintain its temperature constant within 0.1°C. Prior to being fed into the probe the dry carrier gas was brought to the enclosure temperature to minimize heat exchange with the evaporating surface. Thus most of the heat of evaporation was supplied through the water.

Before measurements were made under any particular set of conditions, the probe and the tubes leading to the moisture analyzer were flushed with dry gas to remove all traces of moisture. The water surface was swept with a Teflon bar to remove surface contamination. The probe was then lowered to its position near the surface and dry gas was introduced at a rate of about 1,200 cu. cm./min. The gas leaving the evaporating area through the sampling hole in the center of the probe was withdrawn at a rate of 430 cu. cm./min. and its water concentration was monitored until a steady state was reached, usually in about 30 sec. These flow rates relate to nitrogen, the probe gas for most of the data reported here. Wide variations in flow rates were used in some particular experiments and will be noted.

ANALYSIS OF PROBE BEHAVIOR

Underlying the interpretation of probe measurements by previous investigators were two important assumptions: (1) the flux, whether of water vapor or desorbed gas, which contributes to the observed signal, comes only from the circular surface area, defined by the annular gap of the probe, and is symmetrically distributed over this area; (2) the entire flux from the surface area is incorporated in the gas flow exiting through the central sampling hole. Consequently, the flux per unit surface area could be determined from the concentration of water vapor or desorbed species in the carrier gas and its flow rate. These assumptions seemed so reasonable that their validity was apparently never put to the test by independent direct measurements of actual flux from the surface. Nor was there any analysis or theory of the probe behavior ever presented which could provide any basis for evaluating the experimental results. The present study included both a direct experimental check of the assumptions and a theoretical analysis of transport under the effective probe area. In this section the theory of the probe will be developed.

The model used to represent the geometry is shown in Figure 2. Of the total gas fed to the probe, the fraction which sweeps the evaporating area in a radial, sink-type flow is withdrawn through the center hole at a volume flow rate V. A concentration profile is established between the water surface and the probe. At the surface the mole fraction of the water vapor x_s corresponds to the equilibrium vapor pressure at surface temperature. This statement simply reflects the fact that the resistance for a clean surface is usually very small so that the overall evaporation rate is governed primarily by the surface temperature and the diffusional resistance of the gas.

The following assumptions were made in the derivation:

1. The gas is incompressible and at the same temperature as the water surface. The temperature equality is accomplished in practice by thermostating the dry gas before entering the probe so that no appreciable heat transfer takes place to or from the gas.

2. The velocity profile is unaffected by the mass transfer.

3. Diffusion in the radial direction is much smaller than in direction normal to the surface.

Under these conditions the equation of continuity for water vapor in the carrier gas becomes in cylindrical coordinates

$$u\frac{\partial x}{\partial r} = D\frac{\partial^2 x}{\partial z^2} \qquad (1)$$

The boundary conditions for $r_2 \leq r \leq r_1$ are

$$x(r, 0) = x_s \tag{2a}$$

$$\frac{\partial x}{\partial z}(r, a) = 0 \tag{2b}$$

$$x(r_1, z) = x_1 \tag{2c}$$

The uniformity of the water surface temperature implied by (2a) was confirmed by measurement of water temperatures at different radial positions.

By introducing the variables

$$\eta = \frac{D(r_1^2 - r^2)}{2u_m r_a^2} \tag{3a}$$

$$\zeta = \frac{z}{a} \tag{3b}$$

$$\theta = \frac{x_s - x}{x_s - x_1} \tag{3c}$$

Equation (1) may be made dimensionless into

$$\frac{u}{u_m}\frac{\partial \theta}{\partial \eta} = \frac{\partial^2 \theta}{\partial \zeta^2} \tag{4}$$

where u_m is the average velocity. For a uniform velocity $u/u_m = 1$, while for a fully developed parabolic velocity profile $u/u_m = 6(\zeta - \zeta^2)$. The boundary conditions in dimensionless form become

$$\theta(\eta, 0) = 0$$

$$\frac{\partial \theta}{\partial \zeta}(\eta, 1) = 0$$

$$\theta(0, \zeta) = 1$$

For a uniform velocity profile the solution of (4) is readily available (*14*):

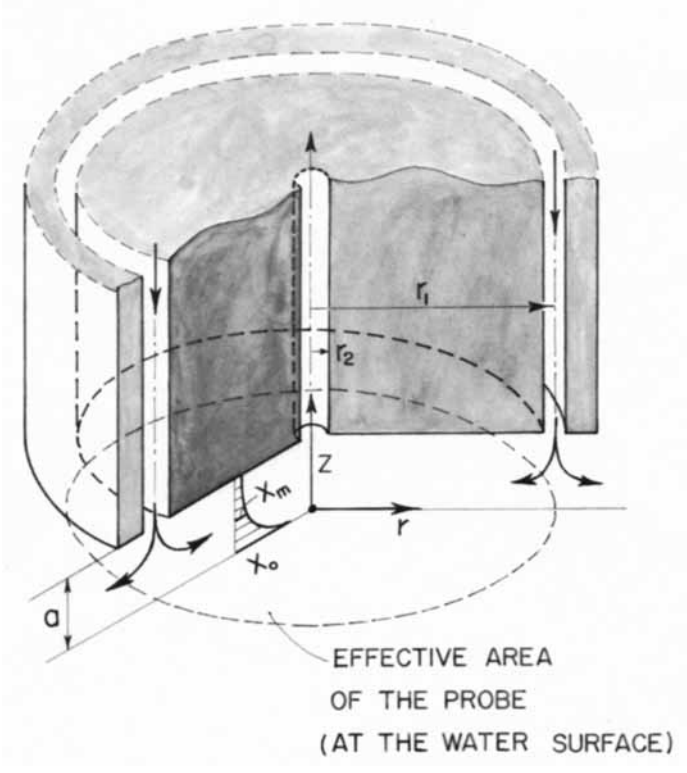

Fig. 2. Flow pattern and water concentration profile under the probe.

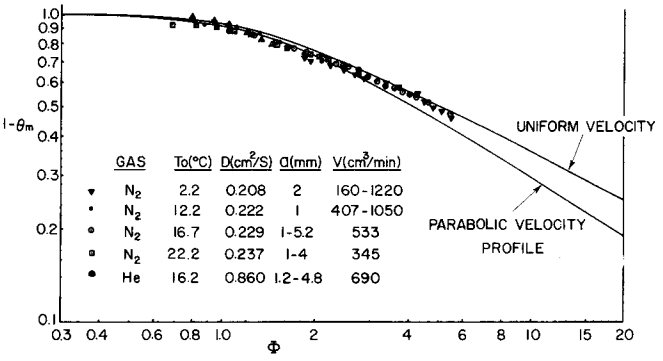

Fig. 3. Average water vapor concentration in the gas. Comparison between theory and experiment at various values of ϕ.

$$\theta = \frac{4}{\pi}\sum_{n=0}^{\infty}\frac{1}{2n+1}\exp -\frac{(2n+1)^2\pi^2}{4}\eta \sin\frac{2n+1}{2}\pi\xi \tag{5}$$

The last expression can be written in a more conventional form by using, instead of η, its reciprocal ϕ:

$$\phi = \frac{Va}{\pi D(r_1^2 - r^2)} = \left(\frac{\nu}{a}\right)\left(\frac{u_m a}{\nu}\right)\frac{2ar_1}{r_1^2 - r^2}$$

$$= N_{Sc} \cdot N_{Re}\frac{2ar_1}{r_1^2 - r^2}$$

It should be noted that N_{Re} depends on r.

The bulk average vapor concentration θ_m, which is defined by

$$\theta_m = \frac{\int_0^1 u\theta\, d\zeta}{\int_0^1 u\, d\zeta}$$

is then obtained from (5) in the form

$$\theta_m = \frac{8}{\pi^2}\sum_{n=0}^{\infty}\frac{1}{(2n+1)^2}\exp -\frac{(2n+1)^2\pi^2}{4\phi} \tag{6}$$

and its magnitude θ_{m_2} upon leaving the probe is obtained when $r = r_2$ or $\phi = \phi_2$.

Measurements of water vapor concentration in the gas leaving the probe were carried out using both nitrogen and helium at different values of V, a, and water temperature. The experimental results are shown in Figure 3 together with the curve calculated from (6) and a curve obtained by numerical integration of (4) for a parabolic velocity profile. For higher values of ϕ the data agree better with the prediction based on uniform velocity. This better agreement is probably due to the fact that the radial gas flow is accelerating and the rate of growth of the boundary layer is small.

The agreement between the analysis and the experiments is comforting because it seems to support the assumptions in the analysis as well as the assumptions mentioned earlier which have been made by previous users of the probe. Moreover, if the theory is correct, it provides, in experiments with this type of probe, a means of estimating the component of overall resistance to mass transfer which is due to diffusion in the gas phase. It becomes feasible therefore to compare results from different investigators even though their experimental conditions may not be identical. For these reasons it was very disconcerting to find that the values for pure water obtained by Walker

(*12*) and by Himmelblau (*13*) did not agree at all with the present results. Walker's operating conditions correspond to a value of ϕ about 0.2. If the curve in Figure 3 is correct, it implies saturation of his sample gas. His reported evaporation data indicate a much lower water concentration, corresponding to about one-third of the evaporation rate predicted by the present theory. Similarly, Himmelblau's data indicate an apparent evaporation rate which is only about 40% of the predicted value. Clearly such disparity requires some explanation.

One possible source of trouble seemed to be in the overall flow rate of gas to the probe and its distribution between the outer curtain flow and the inner sampling flow. For example, if the inner flow is too small, the sampled gas will be saturated and the resistance to evaporation will be due entirely to thermodynamic rather than kinetic effects. Figure 4 shows the results of a series of measurements in which the flow rates were varied. Each curve corresponds to a fixed flow rate of gas through the center hole in the probe. Variations in the abscissa, the ratio of outer to inner flow, were obtained simply by changing the total flow rate to the probe while keeping the center or sampling flow constant. It is clearly desirable to work on the portion of the curve in which the ordinate value is relatively insensitive to the outer flow rate. The conditions of the Walker and Himmelblau experiments correspond to an abscissa value of 0.11, clearly in the region which is very sensitive to flow rate. However, it did not seem likely that this factor could account for all the difference between their results and the present ones.

It became apparent that there was needed some sort of an independent check of the evaporation rate indicated by probe-monitor results. Accordingly, a small container was prepared which could be filled with water and weighed. The exposed surface area could be precisely defined by a cover of plastic foil in which was cut a hole of the desired dimensions. A long series of measurements under a range of conditions with both helium and nitrogen carrier gases left no doubt that in every case the evaporation rate indicated by monitor reading agreed within the experimental error of about 10% exactly with the rate indicated by the weight loss of the container. Moreover, when the exposed surface area was congruent with the effective area of the probe, that is, the circle defined by the annular slot, the weighing results agreed with the probe theory.

This confirmation of the present results was gratifying but there remained an uneasiness because of the disagreement with Walker's and Himmelblau's data. Much time was spent and many exercises were carried out until finally a plausible explanation was found. As it turns out, the degree of symmetry in the gas flow is extremely important. If the inner Teflon cylinder and the outer tube are not exactly concentric, the apparent evaporation rate as indicated by the monitor falls off markedly. When the annular gap through which the dry gas flows is narrowed on one side, there will be a correspondingly higher flow on the opposite, wider side. It may be that there then results an escape of evaporated water into the flow leaving the probe periphery. Such an escape of water vapor is probably what also accounts for the decrease in apparent evaporation rate which shows up at low abscissa values in Figure 4. Thus when the probe is not symmetric the concentration of the gas withdrawn through the center hole does not reflect the true evaporation rate. The possible magnitude of this effect is shown by the following measurements. With helium at the same operating conditions as used by Walker and Himmelblau, and a symmetric probe, the evaporation rate determined from the water loss of the small container was 32×10^{-6} g./(sq. cm.)(sec.). The monitor indicated a rate of 29×10^{-6} g./(sq.cm.)(sec.) When the probe was made eccentric the evaporation rate under the same conditions, as determined from weight loss measurements, was 36×10^{-6} g./(sq.cm.)(sec.) but the monitor reading corresponded to a rate of only 12×10^{-6} g./(sq.cm.)(sec.)! It is noteworthy that the effect of eccentricity on evaporation rate is much greater when the central cylinder is recessed relative to the end of the outer tube. Accordingly, it would seem desirable to keep the ends of the tube and cylinder coplanar. The importance of the three set screws used to adjust and maintain alignment is now obvious. Teflon is especially subject to creep or deformation so that some positive means of centering is highly desirable when it is used. It should be said that insuring symmetry in the probe is most important when absolute values of resistance or rate are required. If only relative values are needed it is probably necessary to be sure only that the probe configuration is the same in each experiment. However, it is just as easy to maintain the correct alignment as to be sure any arbitrary alignment is unchanged. Consequently, correct alignment seems worth striving for. Meanwhile, caution should be exercised in interpreting previous measurements with probes of this type.

HEAT TRANSFER RESULTS

As has been indicated, this study was undertaken as a prerequisite to an investigation of the evaporation-inhibiting properties of monomolecular films. In particular the possible effects of films on natural convection in bulk water were of interest. Accordingly, it was desirable to determine the role of natural convection in the case of pure water with a clean surface. This objective was achieved by a series of measurements in which the temperature of the entire system, the thermostatically controlled enclosure and its contents, including the trough, were cooled to near 0°C. and allowed to warm up slowly. Evaporation rates and temperature profiles were followed as the temperature rose to 22°C. The effect of the transition through 4°C. on the evaporation rate is shown in Figure 5. The rising bulk and surface temperatures of the water during the heating result in a continuously rising evaporation rate. At the bottom temperature T_b of about 4°C. the evaporation rate is enhanced as a result of the onset of buoyancy driven convection in the water. Figure 6 shows the pronounced difference between the tem-

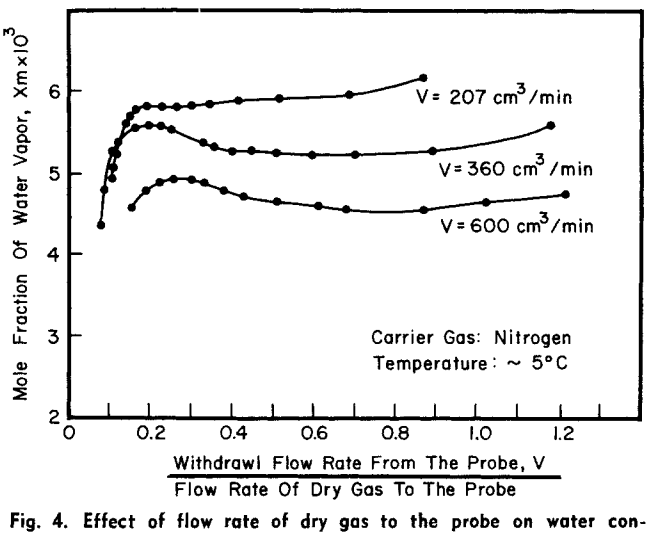

Fig. 4. Effect of flow rate of dry gas to the probe on water concentration in gas withdrawn from the probe.

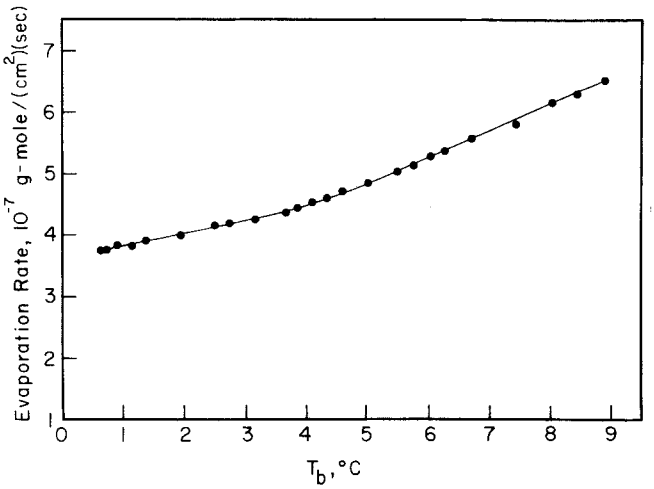

Fig. 5. Effect of raising water temperature and the transition through 4°C. on the evaporation rate.

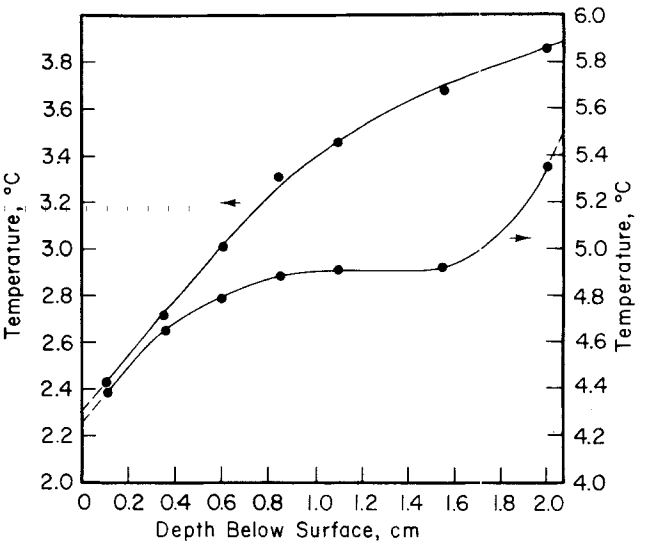

Fig. 6. Typical temperature profiles in the water before and after onset of convection.

perature profiles before and after the onset of convection. The two profiles were recorded under the center of the probe at bottom temperatures T_b of 3.86° and 5.5°C. It is important to note that even with the conductive mode prevailing, the temperature profile is not linear for reasons related to the geometry of the system. Because of restrictions imposed on the design of the trough by its use in subsequent monolayer studies, the thickness of the water layer was of the same order as the diameter of the evaporating area. Consequently, the heat flux to the surface included also a horizontal, or radial, component even in the absence of convection. The steady state vertical temperature distribution could therefore not be linear anywhere under the evaporating area.

The evaporative heat flux q was obtained from the measured evaporation rate and the heat of vaporization. Heat transfer through the water was calculated from the known heat flux and the difference between bottom and surface temperatures $(T_b - T_s)$ under the center of the probe. It was expressed in terms of the Nusselt number, defined by

$$N_{Nu} = \frac{qH}{(T_b - T_s)k} \quad \frac{1}{5.15} \qquad (7)$$

The correction factor 5.15 is the thermal conductance of the water layer under the probe defined as $q_{cond}H/(T_b - T_s)k$, obtained from experiments, in the absence of convection, that is, at temperatures below 4°C. Hence N_{Nu}, as defined above, represents the ratio of the total heat actually transferred through the water to the heat transfer which could be accounted for by conduction. It should be noted that Equation (7) applies directly only to configurations and conditions similar to those used in this work.

A check of the experimental value of the thermal conductance was provided also by theory. The steady state heat conduction was calculated for a slab with one surface at temperature T_b and no heat flow through the other surface, except through a circle maintained at a uniform temperature T_s. With the thickness of the slab and the diameter of the circle taken as the depth of the water layer and the diameter of the evaporating area, respectively, the resulting thermal conductance is 3.23. This model is probably more realistic than that of a cylinder with temperatures T_s at the top surface and T_b at all other boundaries which yielded a thermal conductance of over 8. That the experimental value of 5.15 falls between the results provided by these two idealized models is reassuring. However, it should be noted that the value of 5.15 for the thermal conductance applies only when the ratio of horizontal and vertical components of conductive heat flux is the same as it was in the purely conductive situation for which the conductance was determined. At temperatures above 4°C. when convection occurs the ratio between the two components changes. In all probability the effective values of the conductance will be then less than 5.15. The change in N_{Nu} during the transition through the 4°C. region is shown in Figure 7. The rise in N_{Nu} around $T_b = 4.5$°C. indicates the contribution to heat transfer by natural convection.

It has previously been established theoretically and experimentally that both the onset of convection and the magnitude of the heat transfer thereafter are determined by the Rayleigh number which represents the buoyancy driving force, and is defined by

$$N_{Ra} = \frac{\beta\rho g H^3 \Delta T}{\kappa\mu}$$

where ΔT is the temperature difference across the liquid layer. The determination of N_{Ra} at the onset of convection during a temperature change near 4°C. requires some care. Since a temperature profile exists across the water layer with the lower temperature at the surface, the 4°C. transition temperature can occur inside the liquid at the border between a stable conductive region at the top and an unstable convective region at the bottom. If, following Boger and Westwater (9), the critical N_{Ra} is calculated using for β the highest positive value in the water layer and for ΔT the temperature difference across the layer in which buoyancy exists (that is, $T_b - 4$), the resulting critical N_{Ra} is about 1,500. This is close to the value of 1,100 predicted by the linear stability analysis for a layer of liquid with a free upper surface (15).

At higher water temperatures both evaporation rate and convective heat transfer rate increase as a result of the higher surface temperature. The values of N_{Nu} obtained at various water temperatures above 4°C. are plotted in Figure 7 against N_{Ra}, which is based on water properties at a mean temperature between the bottom and the surface. The results show that N_{Nu} is proportional to $N_{Ra}^{1/3}$ for Rayleigh numbers greater than about 1.5×10^4. A similar functional dependence of N_{Nu} on N_{Ra} has been observed by several investigators over various ranges of N_{Ra}. Results obtained by Federico and Fora-

boschi with water layers exposed at the top (*16*) and by Malkus with water and acetone layers confined between two rigid surfaces (*17*) are shown also in Figure 8. As can be seen the values of N_{Nu} in the present investigation are lower than those of the earlier work. It might be noted that in both previous cases the liquid layer was heated at the bottom rather then cooled at the top. A more likely cause of the difference is the already mentioned horizontal heat flux component which is absent from previous works. As a result the effective value of the thermal conductance in the presence of convection is probably somewhat lower than the value of 5.15 which has been assumed in computing N_{Nu}.

This study shows that measurements with this kind of probe, when appropriately analyzed, can lead to elucidation of the contribution of natural convection to the heat transfer resistance during evaporation. Good use will be made of this result in the interpretation of measurements with monomolecular films which will be reported subsequently.

ACKNOWLEDGMENT

The support of this work under Grant 14-01-0001-438 by the Office of Saline Water, U.S. Department of the Interior, is gratefully acknowledged.

NOTATION

a = distance between the probe and water surface, cm.
D = molecular diffusion coefficient of water in gas phase, sq.cm./sec.
g = gravitational acceleration, cm./sec.^{2}
H = height of water layer, cm.
k = thermal conductivity of water, cal./(sec.)(cm.)(°C.)
N_{Nu} = $qH/(T_b - T_s)k$, Nusselt number, dimensionless
N_{Ra} = $\beta\rho g H^3 \Delta T/\chi\mu$, Rayleigh number, dimensionless
N_{Re} = $u_m a/\nu$, Reynolds number, dimensionless
N_{Sc} = ν/D, Schmidt number, dimensionless
q = heat flux to the water surface, cal/(sq.cm.)(sec.)
r = radial coordinate, cm.
T_s = temperature at water surface, °C.
T_b = temperature at bottom of water layer, °C.
u = radial velocity of the gas, cm./sec.
u_m = average radial velocity of the gas, cm./sec.
V = rate of withdrawal from the probe, cu.cm./sec.
x = mole fraction of the water vapor in gas
z = axial coordinate

Greek Letters

β = volumetric expansion coefficient, 1/°C.
ζ = z/a axial coordinate, dimensionless
η = $D(r_1^2 - r^2)/2u_m r a^2$, radial coordinate, dimensionless
θ = $(x_s - x)/(x_s - x_1)$, concentration, dimensionless
κ = thermal diffusivity, sq.cm./sec.
μ = dynamic viscosity, g./(cm.)(sec.)
ν = kinematic viscosity, sq.cm./sec.
ρ = density, g./cu.cm.

Subscripts

1 = entrance to evaporation area
2 = exit from evaporation area
b = bottom of water layer
m = mean value
s = water surface

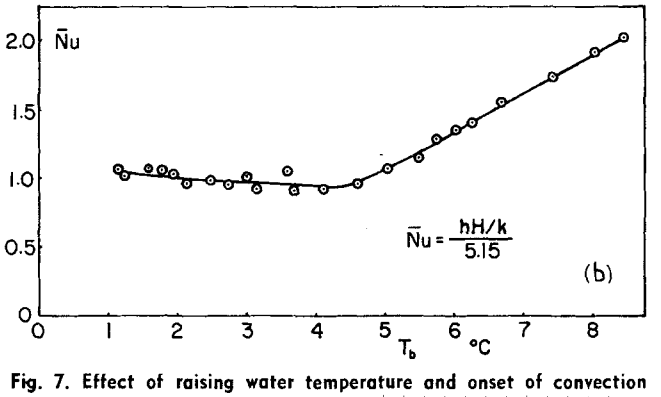

Fig. 7. Effect of raising water temperature and onset of convection on N_{Nu}.

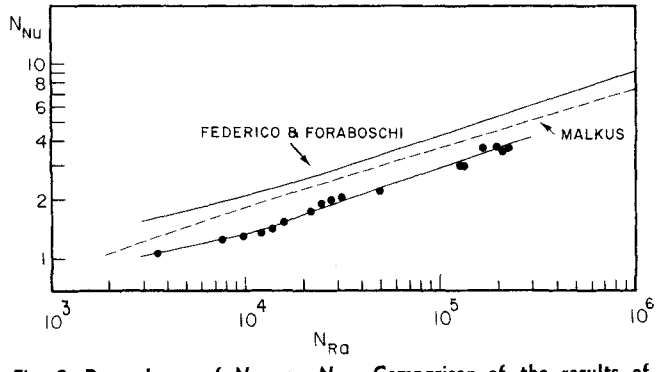

Fig. 8. Dependence of N_{Nu} on N_{Ra}. Comparison of the results of this investigation with other experimental results.

LITERATURE CITED

1. LaMer, V. K., ed., "Retardation of Evaporation by Monolayers: Transport Processes," Academic Press, New York (1962).
2. Langmuir, I., and V. J. Schaefer, *J. Franklin Inst.*, **235**, 119 (1943).
3. Jarvis, N. L., and R. E. Kagarise, *J. Colloid Sci.*, **17**, 501 (1960).
4. Spangenberg, W. G., and W. R. Rowland, *Phys. Fluids*, **4**, 743 (1961).
5. Berg, J. C., M. Boudart, and A. Acrivos, *J. Fluid Mech.*, **24**, 721 (1966).
6. Benard, H., *Rev. Gen. Sci. Pures Appl. Bull. Assoc. Franc. Avan. Sci.*, **11**, 1261 (1900).
7. Goren, S. L., *Chem. Eng. Sci.*, **21**, 515 (1966).
8. Tien, Chen., *AIChE J.*, **14**, 652 (1968).
9. Boger, D. V., and J. W. Westwater, *Trans. ASME J. Heat Transfer*, **89**, 81 (1967).
10. Archer, R. J., and V. K. LaMer, *J. Phys. Chem.*, **59**, 200 (1955).
11. Sebba, F., and H. W. A. Briscoe, *J. Chem. Soc. London*, **106** (1940 I).
12. Walker, D., *Rev. Sci. Instr.*, **34**, 1006 (1963).
13. Sada, E., and D. M. Himmelblau, *AIChE J.*, **13**, 860 (1967).
14. Carslaw, H. S., and J. C. Jaeger, "Conduction of Heat in Solids," 2nd edit., p. 96, Oxford Univ. Press, London (1959).
15. Pellew, A., and R. V. Southwell, *Proc. Roy. Soc.*, **A176**, 312 (1940).
16. Federico, I. D., and F. P. Foraboschi, *Intern. J. Heat Mass Transfer*, **9**, 1351 (1966).
17. Malkus, W. V. R., *Proc. Roy. Soc.*, **A225**, 185 (1964).